



Analytical Study of Concrete Strength Prepared Both from Recycled Concrete Aggregate and Ceramic Aggregate

Uzoukwu S. C., Kareem A. M., Obiora B. C., Ukiwe O. U., Ibeh V. C., Muorah V., Eziefule J. N.

Department of Civil Engineering, School of Engineering and Engineering Technology Owerri, Imo State.

Email: cskambassadors@gmail.com

ABSTRACT:

This study undertakes a comprehensive comparative analysis of concrete made with RCA and ceramic aggregates, focusing on their workability, compressive strength, and bulk density. A total of nine concrete mixtures were prepared, incorporating RCA and ceramic aggregates as partial replacements for natural aggregates. The mixtures were tested for workability, compressive strength, and bulk density at different curing ages. The results showed that concrete made with RCA exhibited superior compressive strength and bulk density, while ceramic aggregate concrete offered improved workability. The curing age was found to have a significant impact on the compressive strength of RCA concrete.

The findings of this study provide valuable insights into the potential of RCA and ceramic aggregates as sustainable alternatives to natural aggregates. The results suggest that RCA concrete may be suitable for structural applications, where high compressive strength is required, while ceramic aggregate concrete may be better suited for non-structural uses, such as decorative concrete or insulation. The study contributes to the development of more sustainable and environmentally friendly construction materials, and provides a foundation for future research on the use of alternative aggregates in concrete production.

Key words: RECYCLED CONCRETE AGGREGATE (RCA), CERAMIC AGGREGATE (C.A)

[A]. Introduction:

The global construction industry heavily relies on concrete, a material that requires vast quantities of natural aggregates such as sand, gravel, and crushed stone. However, the extensive extraction of these natural resources has led to environmental degradation, depletion of natural reserves, and unsustainable mining practices. Additionally, the production of cement, a key ingredient in concrete, contributes significantly to global carbon emissions. These issues have raised concerns about the long-term sustainability of conventional concrete production.

At the same time, the construction and ceramic industries generate large amounts of waste. Demolished concrete structures produce rubble that is often discarded in landfills, while ceramic waste, such as defective tiles and sanitary ware, also contributes to industrial waste. Both types of waste pose serious environmental and waste management challenges, further exacerbating sustainability issues in construction.

Although ceramic waste and recycled concrete aggregates (RCA) have been proposed as alternative materials for replacing natural aggregates in concrete, there are concerns about how these materials impact the mechanical properties of concrete. Ceramic waste tends to have higher porosity and lower density than natural aggregates, while RCA may possess weaker bonds due to residual cement paste, both of which can affect the strength and durability of the final concrete mix. Limited research exists that thoroughly compares the performance of these alternative materials in concrete, especially in terms of their compressive and tensile strength.

Therefore, the problem lies in the insufficient understanding of the impact of ceramic waste and RCA on the strength and performance of concrete. Without reliable data on whether these alternative materials can match or improve upon the strength characteristics of conventional concrete, their adoption in construction remains limited. This study aims to fill this gap by conducting a comparative analysis of the strength of concrete made from ceramic waste and RCA, helping to assess the viability of these materials in promoting sustainable construction practices

B. Objectives of Study

The primary aim of this project is to investigate the strength characteristics of concrete made from ceramic waste and recycled concrete aggregates (RCA) and to compare their performance with that of conventional concrete made with natural aggregates. This study seeks to provide a deeper understanding of the mechanical properties of these alternative materials in concrete, thereby assessing their potential for sustainable construction applications. The specific objectives of the project are as follows:

To investigate some physical properties of the main materials used.

To measure the workability of the concrete.

To measure the bulk density of the concrete.

To determine the compressive strength of the concrete under curing.

To make recommendations with regard to the use of RCA and Ceramic aggregate in concrete production.

Materials

The main materials used for this project were cement, fine aggregate, coarse aggregate, water, and fumed silica.

Cement

For the purpose of this study, Ordinary Portland Cement of Dangote brand, grade 42.5R was used. The cement was sourced from a local retail outlet in Eziobodo, Owerri.

Fine Aggregate

The fine aggregate used for this study was locally available river sand from Otamiri. The river sand was collected in bags and allowed to dry naturally before use. The bulk density was presumed to be 1,560 kg/m³.

Coarse Aggregate

Granite crushed to a maximum aggregate size of 20 mm was used as coarse aggregate. The aggregate was purchased in bags from a local retailer in Obinze, Owerri.

Water

Tap water from the structural laboratory was used in this experiment. The properties are assumed to be equivalent to ordinary water. Specific gravity is taken as 1.00.

Table 1 shows some physical properties of the main materials used in this work.

Materials	Property	Value
Cement	Grade	42.5R
Fine aggregate	Bulk density	1,560 kg/m ³ .
Coarse aggregate	Aggregate size	maximum of 20 mm
Water	Specific gravity	1.00

[C]. Methodology

Determination of Physical Properties of Fine and Coarse Aggregates

For this study, a sieve analysis test was performed on both river sand, crushed granite, ceramic aggregates and RCA to determine their particle size distribution. The test involved utilising a stack of sieves with varying aperture sizes, starting from the largest at the top to the smallest at the bottom.

Representative samples of each aggregate were carefully weighed and placed on the top sieve. The stack was then subjected to mechanical shaking to separate particles based on size. After shaking, the material retained on each sieve was weighed, enabling the calculation of the percentages passing through each sieve.

Apparatus required for the sieve analysis test include: standard sieve sizes with lid and pan, weighing balance, tray, brush, and mechanical sieve shaker.

The test proceeded thus, representative samples of each aggregate (fine and coarse) were carefully weighed and recorded. The weight of each sieve and the pan was also weighed and recorded. The sieves were arranged in ascending order, starting from the smallest at the bottom to the largest at the top as shown in Figure 1. Aggregate samples were then placed on the top sieve and covered with the lid. The stack was then subjected to mechanical shaking for about 10 minutes to separate particles based on size. After shaking, the material retained on each sieve was weighed, enabling the calculation of the percentages passing through each sieve. Figure 3.2 shows the weighing process.



Fig. 1: Manual shaking of the sample in



Fig. 2: Weighing of sample and sievestack sieves

The weight of the soil retained on each sieve was calculated by subtracting the weight of the empty sieve from the recorded weight of the sieve and the sample. The total weights of particles retained were added and compared to the initial weight of the soil sample. The percentage retained on each sieve was determined by dividing each weight retained by the initial weight of the soil sample. Subsequently, the total percentage passing from each sieve was calculated by subtracting the cumulative percentage retained in that particular sieve and the ones above it from totality. The computer data is used to compute the Coefficient of Uniformity (C_u) and the Coefficient of Gradation (C_c), thereafter a graph of sieve sizes against percentage passing through the sieve is plotted to define the gradation of the soil.

No additional preliminary tests were conducted for other main materials, namely Ordinary Portland Cement (OPC), and water. The physical properties of these materials were provided based on established standards and specifications, eliminating the need for further preliminary testing.

Determination of the Workability of Concrete

The following apparatus were used for the slump test: trowel, shovel, weighing balance, tamping rod, oil or grease, brush, slump cone, non-porous base plate, and steel tape.

For a target concrete grade of M15, M20, and M25 and mix ratio of 1:2:4, 1:1.5:3, and 1:1:2 was employed, and a water-cement ratio of 0.55 was used. Batching was done by mass and the material batching data for the various coarse aggregate replacement is shown in Table 2. Values in Table 3 represent the total weight of each concrete component per nine cube mould, and also incorporate a wastage of 15%. Density of concrete made from granite, RCA and ceramic aggregate was taken as $2,400\text{kg/m}^3$, $2,300\text{kg/m}^3$, and $2,200\text{kg/m}^3$ respectively, volume of concrete in 1 mould was calculated to be 0.003375m^3 , and mass of concrete in 1 mould was computed as 8.10kg

The required quantities of each material were measured using a digital weighing scale to ensure accuracy. Three different mix designs were used, with the natural coarse aggregate (granite) replaced by RCA and ceramic aggregate, respectively, for each mix design. The mix designs used were 1:2:4 (cement: fine aggregate: coarse aggregate) for Mix 1 (M15), 1:1:2 for Mix 2 (M20), and 1:1.5:3 for Mix 3 (M25). For each mix design, the natural coarse aggregate (granite) was replaced by RCA and ceramic aggregate, respectively.

Table 2: Material Batching Data for Different Mix Ratios

Mix ratio	Mass of cement (kg)	Mass of Fine Aggregate (kg)	Mass of Natural Aggregate (kg)	Mass of RCA (kg)	Mass of Ceramic Aggregate (kg)	Mass of Water (kg)
1:2:4	7.20	17.00	47.90	45.91	43.92	4.56
1:1:2	12.58	14.85	41.92	40.17	38.42	7.96
1:1.5:3	8.89	16.20	45.73	43.83	41.92	5.65

The dry ingredients (cement, fine aggregate, and coarse aggregate) were mixed together. A shovel was used to mix the ingredients, starting with the cement and fine aggregate as illustrated in Figure 3.3, and then gradually adding the coarse aggregate as in Fig 3.4. The dry ingredients were mixed for approximately 10 minutes, until well combined. The mixing process was done carefully to ensure that all the ingredients were well incorporated and that there were no lumps or unevenness in the mixture. Once the dry ingredients were mixed, the required amount of water was slowly added to the mixture. Water was added using a watering can, and the concrete was mixed using a shovel. Water was added gradually to prevent the mixture from becoming too wet. As the concrete was mixed, its consistency was regularly checked by performing a slump test. The slump test involved filling a cone-shaped mold with the concrete, and then lifting the mold to allow the concrete to slump.

**Fig 3:** concrete mix slump test

Determination of the Bulk Density of Concrete

Apparatus used for the bulk density test include: weighing balance, demoulded and cured cube samples, 150mm x 150mm x 150mm concrete cube moulds, trowel, shovel, tamping rod, oil or grease, brush, bucket or barrow for transporting the samples, and curing tank.

The internal surfaces of the moulds were cleaned and coated with oil to prevent concrete adhesion during hardening as shown in Fig 3.6. Each set of concrete moulds were arranged systematically, providing 9 moulds for each aggregate replacement and for each curing time. The total number of cubes required for the experiment was ascertained thus: 9 cubes for each coarse aggregate replacements (granite, RCA and ceramic aggregate) and 3 cubes for each curing time (7, 14, and 28days), resulting in a total of $9 \times 3 \times 3 = 81$ cubes. Freshly mixed concrete from 3.2.2 was progressively poured into the mould in layers and rammed at least 25 times with the aid of the tamping rod. This process was continued until each mould was adequately filled with concrete. Excess concrete was removed and the cube mould surface levelled using a trowel. The freshly poured concrete was well labelled using a pointed

object to enhance identification of each cube subsequently (refer to Figure 3.6). After a final setting time of 24 hours, the cast concrete cubes were demoulded with utmost care to prevent damage. Demoulded concrete cubes are shown in Figure 3.7 below.



Fig 4: mould preparation



Fig. 5: Freshly mixed concrete cast in cube moulds



Fig. 6: Demoulded concrete cube moulds

Demoulded cubes were subsequently transferred to a curing tank, fully immersed in water, and maintained under controlled temperature and weather conditions as shown in Figure 3.8.

Next, the cube samples were removed from the curing tank after the specified curing period of either 7, 14, or 28 days. The cubes were cleaned of excess water and left to dry for about 1 hour. Using a measuring tape, the dimensions of the cube were taken and used to evaluate the volume of the cube. The mass of each cube was then ascertained using the weighing balance, and recorded alongside the corresponding volume of the cube. The entire procedure was repeated for the different coarse aggregate replacements of natural aggregate with RCA and ceramic aggregate respectively.

The bulk density of the concrete cubes (γ) is the weight per cubic meter of concrete and can be calculated by dividing the weight of hardened concrete by the volume of the concrete cube.

3.2.4 Determination of the Compressive Strength of Concrete

The following equipment were used for the compressive strength test: compression test machine, permanent marker, weighing balance, and cured concrete cube specimen.

The bearing surface of the compression test machine was cleaned and prepared for testing. Cured cube specimen were successively positioned on the compression testing machine and a gradually increasing load was applied to the specimens until they failed. Finally, the maximum load at failure and the corresponding cross-sectional area of the cube were recorded. The entire procedure was then repeated for the rest of the cube specimen associated with different coarse aggregate replacement and curing regimes.

The compressive strength of the concrete cubes can be computed using the following relation:

$$\text{Compressive Strength (fcu)} = (\text{Load at failure}) / (\text{Cross-sectional area of the cube})$$

Mathematically, this can be expressed as:

$$f_{cu} = F / A$$

where:

- f_{cu} = Compressive strength of the concrete cube (in N/mm² or MPa)

- F = Load at failure (in N or kN)

- A = Cross-sectional area of the cube (in mm²)

[E]. Results

Test results for the various methods carried out to achieve the objectives of the research are presented below under appropriate headings.

Determination of Physical Properties of Fine and Coarse Aggregates

Table 3 shows the sieve analysis test results on fine aggregates used in the research work. The particle size distribution curve is shown in Figure 3 illustrating the values for D₆₀, D₃₀, and D₁₀ which are used in determining the Coefficient of Uniformity (Cu) and the Coefficient of Gradation (Cc) of the soil. The weights of the empty pan and the initial aggregate sample were obtained as 299.40g and 552.50g respectively.

Table 3: Sieve Analysis Test Results for Fine Aggregates

Sieve Size (mm)	Weight of empty sieve (g)	Weight of sieve and sample (g)	Weight of sample retained (g)	Percentage retained (%)	Cumulative percentage retained (%)	Cumulative percentage passing (%)
4	547.4	553.08	5.68	1.03	1.03	98.97
2.36	536.25	548.91	12.66	2.29	3.32	96.68
1.18	365.84	420.16	54.32	9.83	13.15	86.85
0.6	359.78	537.2	177.42	32.11	45.26	54.74
0.3	351.16	592.99	241.83	43.77	89.03	10.97
0.15	339.46	389.79	50.33	9.11	98.14	1.86
0.075	337.77	346.46	8.69	1.57	99.72	0.28
Pan	299.4	300.78	1.38	0.25	100.00	0.00

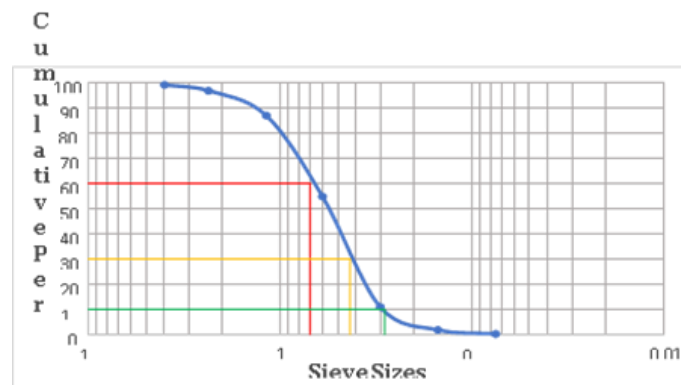


Fig 7: Particle Size Distribution Curve For Fine Aggregates

From Figure 4.1, it can be deduced using computer analysis that:

$$D_{60} = 0.695$$

$$D_{30} = 0.430$$

$$D_{10} = 0.284$$

$$\text{Coefficient of Uniformity (Cu)} = D_{60}/D_{10}$$

Where:

- D60 = Diameter of the particles at which 60% of the material is finer

- D10 = Diameter of the particles at which 10% of the material is finer

Therefore,

$$Cu = \frac{D_{60}}{D_{10}} = \frac{0.695}{0.284} = 2.45$$

Also,

$$\text{Coefficient of gradation (Cc)} = (D_{30})^2 / (D_{60} * D_{10})$$

Where:

- Cc = Coefficient of gradation

- D30 = Diameter of the particles at which 30% of the material is finer

- D60 = Diameter of the particles at which 60% of the material is finer

- D10 = Diameter of the particles at which 10% of the material is finer

Therefore,

$$Cc = \frac{(D_{30})^2}{D_{60} * D_{10}} = \frac{0.430^2}{0.695 * 0.284} = 0.94$$

Table 4 shows the sieve analysis test results on coarse aggregates used in the research work. The particle size distribution curve is also shown in Figure 8, illustrating the values for D60,

D30, and D10 which are used in determining the Coefficient of Uniformity (Cu) and the Coefficient of Gradation (Cc) of the soil. The weights of the empty pan and the initial aggregate sample were obtained as 299.40g and 705.46g respectively.

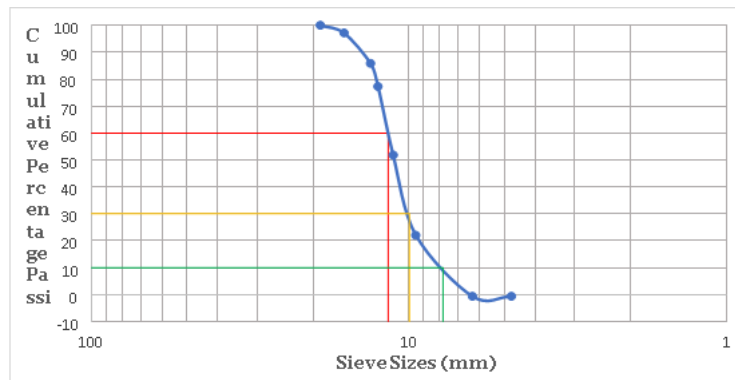


Fig 8: Particle Size Distribution Curve for Coarse Aggregates

From Figure 8, it can be deduced using computer analysis that:

$$D_{60} = 11.62$$

$$D_{30} = 9.95$$

$$D_{10} = 7.80$$

Therefore,

$$\text{Coefficient of Uniformity (Cu)} = \frac{D_{60}}{D_{10}} = \frac{11.62}{7.80} = 1.49$$

Also,

$$Coefficient\ of\ Gradation\ (Cc) = \frac{D_{30}^2}{D_{60} \times D_{10}} = \frac{9.95^2}{11.62 \times 7.80} = 1.09$$

Determination of the Workability of Concrete

Table 4 shows the results of the slump test carried out on concrete with various coarse aggregate replacements for different Mix Ratios.

Table 4: Test Results of Concrete Slump in mm

Mix Ratio	Traditional Concrete	RCA	Ceramic aggregate
1:2:4	23.4	17.4	21.8
1:1:2	21.6	20.7	24.7
1:1.5:3	19.2	21.2	26

Determination of the Bulk Density of Concrete

Table 4: shows the Bulk density of concrete with natural aggregates,

RCA and ceramic aggregate after 7 days of curing

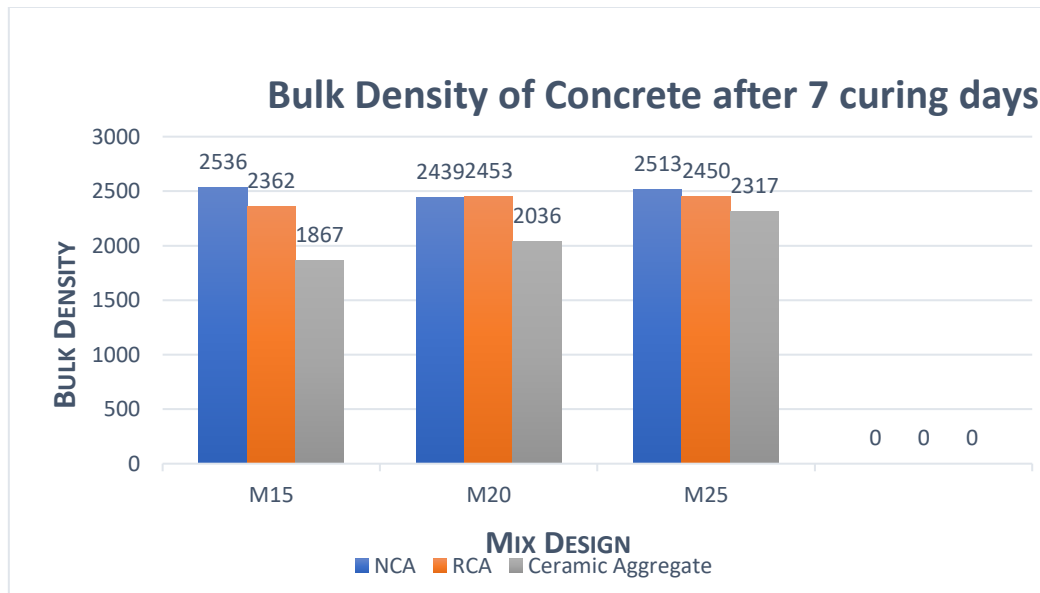


Figure 9: Bulk Density of Concrete after 7 curing days.

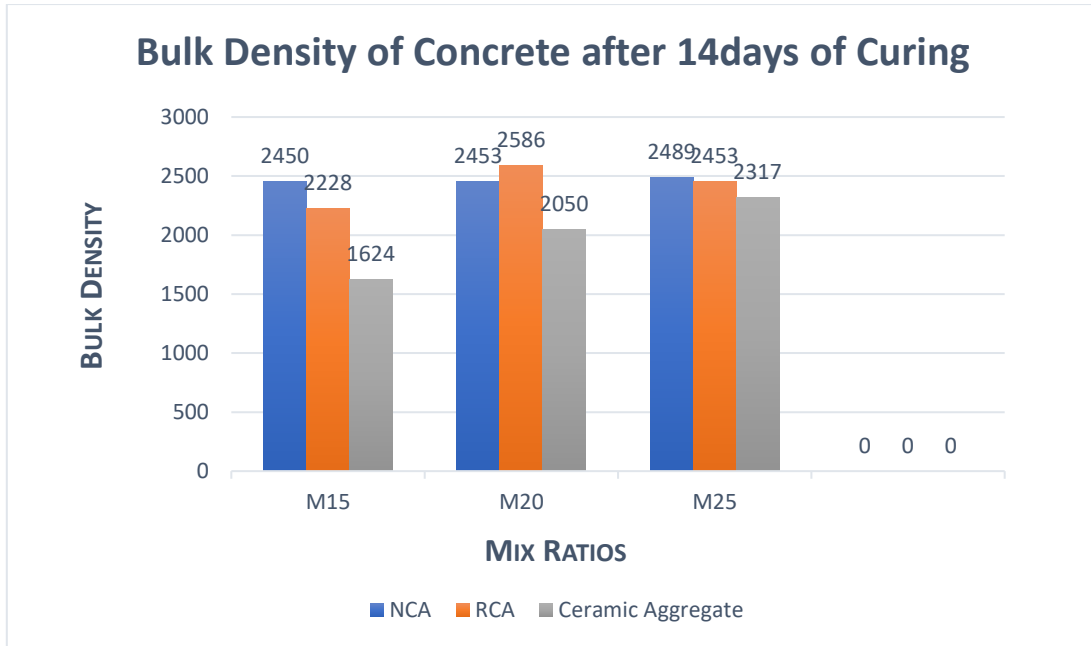


Figure 10: Bulk Density of Concrete after 14days of Curing.

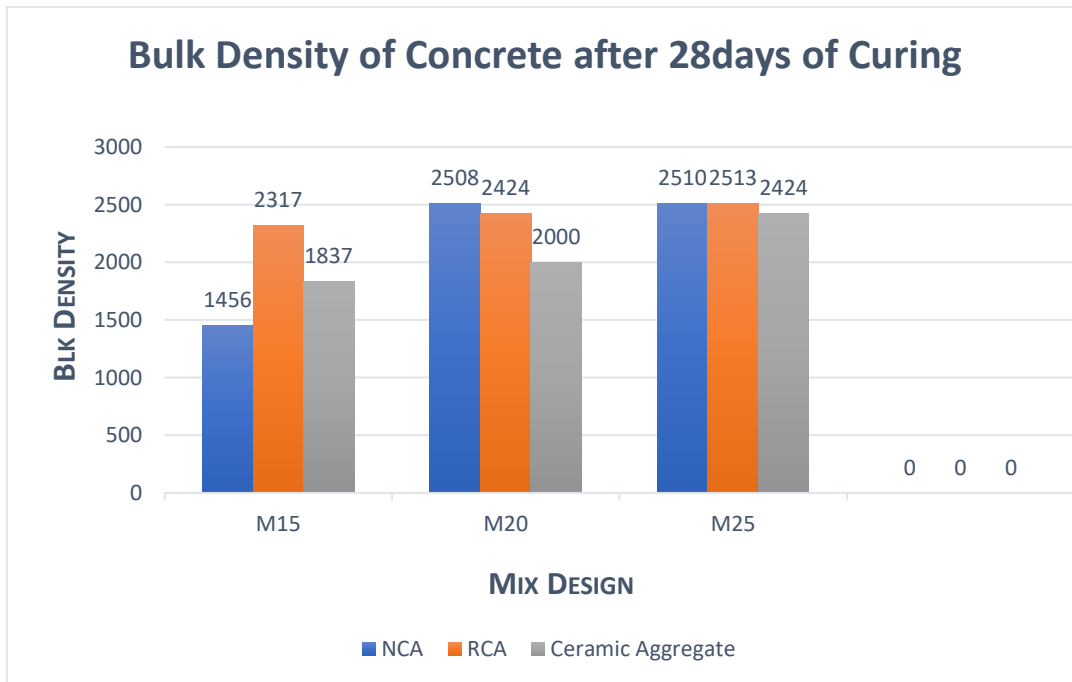


Figure 11: Bulk Density of Concrete after 28days of Curing.

Determination of the Compressive Strength of Concrete

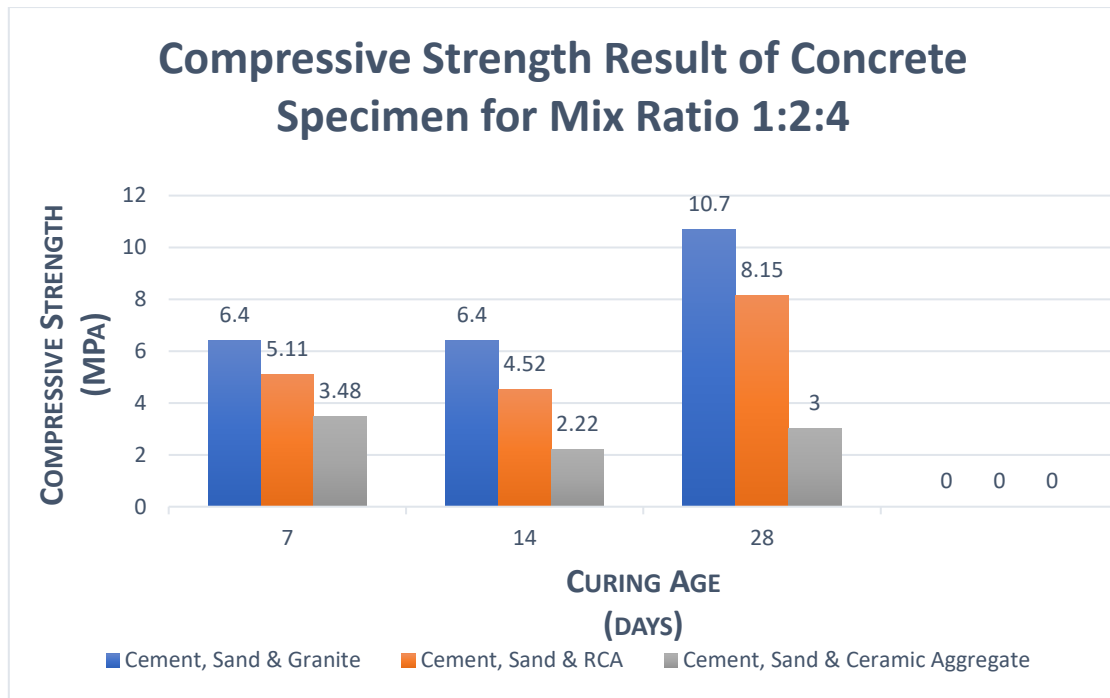


Figure 12: Compressive Strength Result of Concrete Specimen for Mix Ratio 1:2:4.

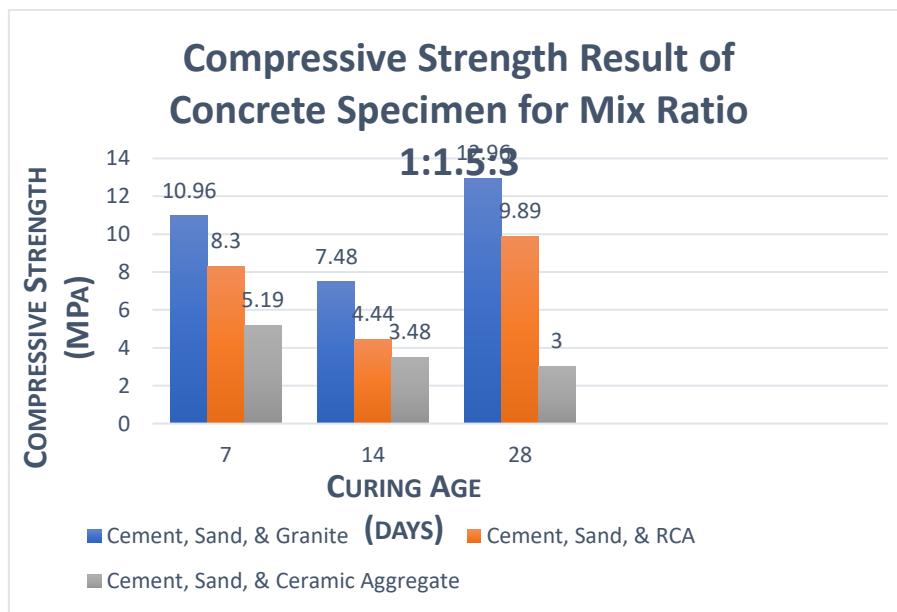


Figure 13: Compressive Strength Result of Concrete Specimen for Mix Ratio 1:1.5:3.

Discussion of Results

This section includes a detailed analysis and interpretation of the results obtained from the various tests carried out to achieve the objectives of the research.

Determination of the Physical Properties of Fine and Coarse Aggregates

The fairly S-shape of the particle size distribution curve, indicates that the fine aggregate used for the research possesses a small range of particles, suggesting a poorly graded sand. Coefficient of uniformity (Cu) and coefficient of gradation (Cc) have been evaluated as 2.45 and 0.94 respectively, both values indicating that the soil specimen has fair distribution of soil particle sizes, good stability, tight packing, and drainage.

The shape of the particle size distribution curve, connotes a uniformly graded soil. This implies that the coarse aggregates used for the research have particles of almost the same size. This is further confirmed by its coefficient of uniformity (Cu) of 1.49 and coefficient of gradation (Cc) of 1.09.

Nonetheless, the distribution of soil particles suggests that both fine and coarse aggregate specimen are suitable for use in concrete production and testing.

Determination of the Workability of Concrete

Slump values are indicative of the ease with which the concrete mix will flow and fill a mould, depending on the aggregate substitute in the concrete. All the slump values fall between 17–30mm indicating a low workability mix, which requires more effort to handle and spread. Such concrete mixes are suitable for foundations, beams, columns with light reinforcement.

It can also be deduced from the trend of slump values that the ceramic aggregate exhibits higher slump values compared to the traditional concrete (granite) and RCA for all mix designs. This suggests that the ceramic aggregate may improve the workability of the concrete. The use of RCA as a substitute for granite appears to affect the workability of the concrete, with lower slump values observed for Mix Design 1:2:4. However, for Mix Designs 1:1:2 and 1:1.5:3, the RCA shows comparable or higher slump values compared to the traditional concrete (granite).

Determination of the Bulk Density of Concrete

At 7 days of curing the bulk density values for the traditional concrete (granite) are the highest, ranging from 8.23 kg/m³ to 8.56 kg/m³. The RCA and ceramic aggregate show lower bulk density values, ranging from 7.97 kg/m³ to 8.28 kg/m³ and 6.30 kg/m³ to 7.82 kg/m³, respectively. As the curing age increases to 14 days, the bulk density values for the traditional concrete (granite) remain relatively stable, ranging from 8.27 kg/m³ to 8.40 kg/m³. The RCA shows a slight decrease in bulk density values, ranging from 7.52 kg/m³ to 8.28 kg/m³. The ceramic aggregate shows a significant decrease in bulk density values, ranging from 5.48 kg/m³ to 7.82 kg/m³. At 28 days of curing, the bulk density values for the traditional concrete (granite) remain relatively stable, ranging from 8.32 kg/m³ to 8.47 kg/m³. The RCA shows a slight increase in bulk density values, ranging from 7.82 kg/m³ to 8.48 kg/m³. The ceramic aggregate shows a slight increase in bulk density values, ranging from 6.20 kg/m³ to 8.18 kg/m³.

Overall, the results indicate that the traditional concrete (granite) exhibits the highest bulk density values across all curing ages. The RCA shows relatively stable bulk density values, while the ceramic aggregate shows a significant decrease in bulk density values at 14 days of curing. The use of RCA and ceramic aggregate as substitutes for granite appears to affect the bulk density of the concrete. The RCA shows a slight decrease in bulk density values, while the ceramic aggregate shows a significant decrease. This may be due to the differences in density and porosity of the aggregates. The results suggest that the mix design and aggregate type have a significant impact on the bulk density of the concrete.

Determination of the Compressive Strength of Concrete

A notable trend emerges, where the traditional concrete mixture, comprising granite, consistently exhibits superior compressive strength across all mix designs and curing ages. In contrast, the mixtures incorporating recycled concrete aggregate (RCA) and ceramic aggregate demonstrate reduced compressive strength. This disparity is particularly pronounced in the case of ceramic aggregate, which exhibits significantly lower compressive strength values.

The variation in compressive strength can be attributed to the distinct properties of each aggregate type. Granite, being a natural, high-strength aggregate, contributes to the superior compressive strength of the traditional concrete mixture. Conversely, the RCA and ceramic aggregate, with their inherently lower strengths and potential for increased porosity, compromise the compressive strength of the concrete.

Another aspect worth exploring is the influence of mix design on compressive strength. The results suggest that the 1:1.5:3 mix design, which incorporates a higher cement content, yields the highest compressive strength values among the traditional concrete mixtures. However, this trend is not consistently observed across the RCA and ceramic aggregate mixtures, indicating that the interplay between mix design and aggregate type is complex and warrants further investigation.

[E]. CONCLUSIONS

The investigation into the effects of using recycled concrete aggregate (RCA) and ceramic aggregate as substitutes for granite in concrete production has yielded valuable insights. The results indicate that the use of RCA and ceramic aggregate can significantly affect the compressive strength, workability, and bulk density of concrete. However, the extent to which these effects are beneficial or detrimental remains a subject of ongoing research.

From the results and analysis discussed so far, the following conclusions were drawn about the research:

- i. The compressive strength of concrete decreases with the use of RCA and ceramic aggregate as substitutes for granite.
- ii. The workability of fresh concrete mix is affected by the type of aggregate used, with ceramic aggregate exhibiting higher slump values.
- iii. The bulk density of concrete is influenced by the curing age, with longer curing regimes resulting in higher bulk density values.
- iv. The mix design has a significant impact on the compressive strength of concrete, with the 1:1.5:3 mix design yielding the highest compressive strength values.
- v. The use of RCA and ceramic aggregate as substitutes for granite may not be suitable for structural applications, but may be suitable for non-structural applications or specialized uses.

[F]. RECOMMENDATIONS

In order to further explore the potential of using RCA and ceramic aggregate in concrete production, the researcher recommends:

- i. Conducting further research on the long-term durability and sustainability of concrete mixtures incorporating RCA and ceramic aggregate.
- ii. Investigating the effects of using RCA and ceramic aggregate on the tensile and flexural strength of concrete.
- iii. Exploring alternative mix designs and curing regimes to optimize the performance of concrete mixtures incorporating RCA and ceramic aggregate.
- iv. Developing guidelines and standards for the use of RCA and ceramic aggregate in concrete production.
- v. Conducting education and training programs to raise awareness among engineers, contractors, and builders about the benefits and limitations of using RCA and ceramic aggregate in concrete production.

[G. REFERENCES

- ACI Committee 301: *Specifications for Structural Concrete*. Available at www.concrete.org.
- ACI Committee 308. (2014). *Guide to Curing Concrete (ACI 308R-01)*. American Concrete Institute.
- Adeyuyi, A. P., & Ola, B. F. (2005). Application of waterworks sludge as partial replacement for cement in concrete production. *Science Research Essays*, 4(4), 190-195.
- Alam, T. *Main Properties of Concrete for Production*. Civil Today. <https://civiltoday.com/civil-engineering-materials/concrete/338-properties-ofconcrete>.
- ASTM International. (2017). *Standard Specification for Chemical Admixtures for Concrete*. ASTM C494.
- Bentz, D. P., et al. (2011). "The role of pozzolans in the hydration of Portland cement." *Cement and Concrete Research*, 41(6), 590-598.
- Bhanja, S., & Sengupta, B. (2016). "Effect of superplasticizers on the properties of concrete." *Construction and Building Materials*, 105, 395-403.
- Bhasin, A., & Singh, S. (2014). "Impact of quarrying on the environment." *International Journal of Environmental Science and Development*, 5(2), 177-182.
- Bola, A. I., et al. (2021). "Utilization of fly ash as a partial cement replacement in concrete: A review." *Journal of Building Materials and Structures*, 8(1), 1-9.
- Department of Materials Science and Engineering, University of Illinois Urbana-Champaign (UIUC) (1995). *Concrete: A Material for the New Stone Age*. Materials Science and Technology (MAST) Module. Archived (PDF) from the original on 9th January 2024.
- Etxeberria, M., Vázquez, E., Marí, A., & Barra, M. (2007). "Influence of amount of recycled coarse aggregates and production process on properties of recycled aggregate concrete." *Cement and Concrete Research*, 37(5), 735-742.
- Faleschini, F., Zanini, M. A., & Pellegrino, C. (2016). Recycled concrete containing ceramic aggregates: Mechanical and durability properties. *Construction and Building Materials*, 128, 248-258.

$$fw_y^1 = 2n_2 + 3n_3 + 4n_4 + 5n_5 = -\frac{1n_5}{5} \quad 34$$

Further simplifying Equation 34 gives

$$n_2 = \frac{-3n_3 - 4n_4 - 5n_5 - \frac{1n_5}{5}}{2} \quad 35$$

Also for the second derivative of the deflection on the X axis,

$$fw_x^{11} = 0 = 0 + 2n_2 + 6n_3 + 12n_4 + 20n_5 \quad 36$$

rearranging the equation and making n_3 the subject gives

$$2n_2 = -6n_3 - 12n_4 - 20n_5 \quad 37$$

in simpler form as

$$n_2 = -3n_3 - 6n_4 - 10n_5 \quad 38$$

Solving for the third derivative of the deflection on the horizontal component gives

$$fw_x^{111} = 0 = 6n_3 + 24n_4 + 60n_5 \quad 39$$

That is

$$fw_x^{111} = 0 = n_3 + 4n_4 + 10n_5 \quad 40$$

$$n_3 = -10n_5 - 4n_4 \quad 41$$

Resolving Equation 35 and 38 together gives

$$\frac{-3n_3 - 4n_4 - 5n_5 - \frac{1n_5}{5}}{2} = -3n_3 - 6n_4 - 10n_5 \quad 42$$

and further simplifying gives

$$-1.5n_3 - 2n_4 - 2.6n_5 = -3n_3 - 6n_4 - 10n_5 \quad 43$$

Bringing the like terms together

$$1.5n_3 + 4n_4 + 7.4n_5 = 0$$

$$n_3 = \frac{-4n_4 - 7.4n_5}{1.5} \quad 44$$

Further simplification gives

$$n_3 = -2.66667n_4 - 4.93333n_5 \quad 45$$

Solving Equations 41 and Equation 45 together gives

$$-10n_5 - 4n_4 = -2.66667n_4 - 4.93333n_5 \quad 46$$

Collecting the like terms together gives

$$-4n_4 + 2.66667n_4 = 10n_5 - 4.93333n_5 \quad 47$$

$$-1.33333n_4 = 5.06667n_5$$

$$\text{That means } n_4 = \frac{5.06667}{-1.33333}n_5 = -3.73337n_5 \quad 48$$

In order to obtain the values of the n_2 and n_3 interms of n_5 , substitute

Equation 48 into Equation 45 and 35 and gives

$$n_3 = -2.66667(-3.73337n_5) - 4.93333n_5$$

$$n_3 = 9.955666n_5 - 4.93333n_5$$

$$n_3 = 9.955666n_5 - 4.93333n_5 = 5.022366n_5 \quad 49$$

$$n_2 = \frac{-3(5.022366n_5) - 4(-3.73337n_5) - 5n_5 - \frac{1n_5}{5}}{2}$$

$$n_2 = \frac{-15.0671n_5 + 14.9333n_5 - 85n_5 - 0.2n_5}{2}$$

$$n_2 = -2.667n_5 \text{ or } -2.7n_5 \quad 50$$

Similarly when Equations 50, 49 and 48 substituted back into Equation 25, that gives

$$\begin{aligned} fw_y &= (-2.7n_5J^2 + 5.02n_5J^3 - 3.7n_5J^4 + n_5J^5) \\ &= n_5(2.7J^2 - 5.02J^3 + 3.7J^4 - J^5) \end{aligned} \quad 51$$

when multiplied by negative one.

Then the Shape function is expressed as

$$fw = m_5 n_5 (2.7I^2 - 5.02I^3 + 3.7I^4 - I^5) * (2.7J^2 - 5.02J^3 + 3.7J^4 - J^5) \quad 52i$$

The Bucking Analysis

The shape functions were further differentiated at different stages, and the

integration of the differential values gave the stiffness coefficients. These includes

$$f = (2.7I^2 - 5.02I^3 + 3.7I^4 - I^5) * (2.7J^2 - 5.02J^3 + 3.7J^4 - J^5)$$

$$\frac{\partial f}{\partial I} = (5.4I + 15.06I^2 - 15.2I^3 + 5I^4)(2.7J^2 - 5.02J^3 + 3.7J^4 - J^5) \quad 52ii$$

$$\frac{\partial^2 f}{\partial I \partial J} = (5.4I + 15.06I^2 - 15.2I^3 + 5I^4)(5.4J + 15.06J^2 - 15.2J^3 + 5J^4) \quad 52iii$$

$$\frac{\partial^3 f}{\partial I \partial J^2} = (5.4I + 15.06I^2 - 15.2I^3 + 5I^4)(5.4 + 15.06J^2 - 15.2J^3 + 5J^4) \quad 53$$

$$\frac{\partial^2 f}{\partial I^2} = (5.4 + 30.12I - 45.6I^2 + 20I^3)(2.7J^2 - 5.02J^3 + 3.7J^4 - J^5) \quad 54$$

$$\frac{\partial^3 f}{\partial I^3} = (30.12 - 91.2I + 60I^2)(2.7J^2 - 5.02J^3 + 3.7J^4 - J^5) \quad 55$$

also

$$\frac{\partial f}{\partial J} = (2.7I^2 - 5.02I^3 + 3.7I^4 - I^5) * (5.4J + 15.06J^2 - 15.2J^3 + 5J^4) \quad 56$$

$$\frac{\partial^2 f}{\partial J^2} = (2.7I^2 - 5.02I^3 + 3.7I^4 - I^5) (5.4 + 30.12J - 45.6J^2 + 20J^3) \quad 57$$

$$\frac{\partial^3 f}{\partial J^3} = (2.7I^2 - 5.02I^3 + 3.7I^4 - I^5) (30.12 - 91.2J + 60J^2) \quad 58$$

Integrating the product of the Equation 55 and 50 gives the first stiffness coefficient.

That is

$$k_1 = \int_0^1 \int_0^1 \frac{\partial^3 f}{\partial I^3} * \frac{\partial f}{\partial I} dIdJ \quad 59$$

$$k_1 = \int_0^1 \int_0^1 [(30.12 - 91.2I + 60I^2)(2.7J^2 - 5.02J^3 + 3.7J^4 - J^5) * (5.4I + 15.06I^2 - 15.2I^3 + 5I^4)(2.7J^2 - 5.02J^3 + 3.7J^4 - J^5)] dIdJ \quad 60$$

bringing the like terms together gives

$$= \int_0^1 \int_0^1 [(30.12 - 91.2I + 60I^2)5.4I + 15.06I^2 - 15.2I^3 + 5I^4) * (2.7J^2 - 5.02J^3 + 3.7J^4 - J^5)(2.7J^2 - 5.02J^3 + 3.7J^4 - J^5)] dIdJ \quad 61$$

further minimization and substitution of the upper and lower limits yields

$$k_1 = 0.15792$$

also integrating the product Equation 53 and 51 give the second stiffness coefficient.

That is

$$k_2 = \int_0^1 \int_0^1 \frac{\partial^3 f}{\partial I \partial J^2} * \frac{\partial f}{\partial I} dIdJ \quad 62$$

Fixing the real values gives

$$k_2 = \int_0^1 \int_0^1 [(5.4I + 15.06I^2 - 15.2I^3 + 5I^4)(5.4 + 15.06J^2 - 15.2J^3 + 5J^4) * (5.4I + 15.06I^2 - 15.2I^3 + 5I^4)(2.7J^2 - 5.02J^3 + 3.7J^4 - J^5)] dIdJ \quad 63$$

Bring the like terms together gives

$$\int_0^1 \int_0^1 [(5.4I + 15.06I^2 - 15.2I^3 + 5I^4)(5.4I + 15.06I^2 - 15.2I^3 + 5I^4) * (5.4 + 15.06J^2 - 15.2J^3 + 5J^4)(2.7J^2 - 5.02J^3 + 3.7J^4 - J^5)] dIdJ \quad 64$$

Multiplying and further integrating the differential values gives

$$k_2 = 0.035689 \quad 65$$

Furthermore integrating the product Equation 58 and 56 give the third stiffness coefficient.

That is

$$k_3 = \int_0^1 \int_0^1 \frac{\partial^3 f}{\partial J^3} * \frac{\partial f}{\partial J} dIdJ \quad 66$$

$$k_3 = \int_0^1 \int_0^1 [(2.7I^2 - 5.02I^3 + 3.7I^4 - I^5)(30.12 - 91.2J + 60J^2) * (2.7I^2 - 5.02I^3 + 3.7I^4 - I^5) * (5.4J + 15.06J^2 - 15.2J^3 + 5J^4)] dIdJ \quad 67$$

$$k_3 = \int_0^1 \int_0^1 [(2.7I^2 - 5.02I^3 + 3.7I^4 - I^5)(2.7I^2 - 5.02I^3 + 3.7I^4 - I^5) * (30.12 - 91.2J + 60J^2)(5.4J + 15.06J^2 - 15.2J^3 + 5J^4)] dIdJ \quad 68$$

integrating Equation 65 and introducing the upper and lower limits gives

$$k_3 = 0.15792$$

and finally integrating the product Equation 51 and 51 gives the sixth stiffness coefficient.

That is

$$k_6 = \int_0^1 \int_0^1 \left(\frac{\partial f}{\partial I} * \frac{\partial f}{\partial I} \right) dIdJ \quad 69$$

That is

$$k_6 = \int_0^1 \int_0^1 [(5.4I + 15.06I^2 - 15.2I^3 + 5I^4)(2.7J^2 - 5.02J^3 + 3.7J^4 - J^5) * (5.4I + 15.06I^2 - 15.2I^3 + 5I^4)(2.7J^2 - 5.02J^3 + 3.7J^4 - J^5)] dIdJ \quad 70$$

Collecting the like terms together gives

$$= \int_0^1 \int_0^1 [(5.4I + 15.06I^2 - 15.2I^3 + 5I^4)(5.4I + 15.06I^2 - 15.2I^3 + 5I^4) * (2.7J^2 - 5.02J^3 + 3.7J^4 - J^5)(2.7J^2 - 5.02J^3 + 3.7J^4 - J^5)] \, dI \, dJ$$

71

Putting the upper and lower limit values gives

$$k_6 = 0.011423$$

Reducing Equation (xiii) in terms of the stiffness coefficients gives

$$B_{klv} = \frac{D(kccff_1 + 2\frac{1}{p^2}kccff_2 + \frac{1}{p^4}kccff_3)}{kccff_6 m^2} \tag{65}$$

Substituting the real values in to Equation 65 gives

$$b_{klv} = \frac{D(0.15792 + 2\frac{1}{p^2}0.035689 + \frac{1}{p^4}0.15792)}{0.011423m^2} \tag{66}$$

Results: The values of the coefficients and the buckling load coefficients were derived. Taking into account the critical buckling load coefficients at different aspect ratios, the values of the buckling loads were all derived. The first table represents the values of the stiffness coefficients while the other contains the critical buckling coefficients for the aspect ratio of m/n, both for the previous and present study..

Table 1.1 Stiffness Coefficients from present work/previous researchers

Stiffness coeffi., k	Present Work	Previous Work
k ₁	0.1579	0.1580
k ₂	0.0356	0.0357
k ₃	0.15782	0.1585
k ₆	0.011323	0.01134

Table 1.2 Critical buckling load values for C-C-F-F plate from previous/present.

m/n		2	1.9	1.8	1.7	1.6
B		42.9346	43.0759	43.2415	43.4373	43.6711
B _x	Previous	43.3728	43.5151	43.6826	43.8814	44.1201
	Present	43.9346	44.0759	44.2415	44.4373	44.6711

Table 1.2 cont'd.

m/n		1.5	1.4	1.3	1.2	1.1	1
B		43.953	44.298	44.726	45.267	45.9632	46.88
B _x ^G / _n ²	Previous	44.410	44.767	45.214	45.785	46.5315	47.531
	Present	44.953	45.298	45.726	46.267	46.9632	47.88

Discussion:

The values of the aspect ratios ranges from 2.0 to 1.0 with arithmetic increase of 0.1. From the values generated in the tables, it was observed that as the aspect ratio increases from 1.0 to 2.0, the critical buckling load decreases. This occurred both in the present and previous results and so in both cases showing an inverse relationship to each other.

References:

[1] Shinde, B.M., Sayyad, A.S. & Kowade, A.B. (2013). Thermal Analysis Of Isotropic Plates Using Hyperbolic Shear Deformation Theory. *Journal of Applied and Computational Mechanics* 7 (2013) 193-204

[2] Da-Guang Zhang (2014). "Nonlinear Bending Analysis of FGM Rectangular Plates with Various Supported Boundaries Resting on Two-Parameter Elastic". *Archive of Applied Mechanics*. Vol. 84, Issue: 1, Pp.1 -20

-
- [3] An-Chien W., Pao-Chun L. and Keh-Chynan, T. (2013). "High – Mode Buckling-restrained Brace Core Plates". Journals of the International Association for Earthquake Engineering.
- [4] Ali Reza Pouladkhan (2011). "Numerical Study of Buckling of Thin Plate". International Conference on Sustainable Design and Construction Engineering. Vol. 78, Issue: 1, Pp. 152 – 157.
- [5] Singh, S.K & Chakrabarti, A. (2012). Buckling Analysis of Laminated Composite Plates Using an Efficient C⁰FE Model. *Latin American Journal of Solids and Structures*. Soni, S.R. (1975), *Vibrations of Elastic Plates and Shells of Variables Thickness*. Ph.D. Thesis. University of Roarkee.
- [6] Srinivasa, C.V., Suresh, Y.J. and Prema, W.P. (2012). "Buckling Studies on Laminated Composite Skew Plate". *International Journal of Computer Applications*. Vol. 37, Issue:1, Pp. 35-47.